AIAA JOURNAL
Vol. 47, No. 5, May 2009

Simulation and Optimization of Flow Control Strategies for Novel High-Lift Configurations

M. Meunier*
ONERA, 92190 Meudon, France

DOI: 10.2514/1.38245

A kriging-based optimization algorithm is presented and applied to the design of a novel high-lift airfoil with a simply hinged, slotless flap and equipped with fluidic flow control. The position, orientation, and continuous-blowing characteristics of the actuator are set as design variables for the maximization of lift in landing conditions. Comparisons with a fully slotted reference configuration are presented and conclusions are drawn. In particular, it is found that a careful parameterization of the jet is capable of an efficient control strategy and leads to a complete reattachment of the flap flow, with considerable gains in lift and aerodynamic efficiency. A functional analysis of variance demonstrates the possibility of a dimensional reduction in the problem formulation and allows for a more in-depth analysis of the mechanisms governing separation management and alleviation in that particular case.

Nomenclature

C_l	=	lift coefficient
C_p	=	pressure coefficient
C_μ	=	jet momentum coefficient
$E[I(.)]$	=	expected improvement criterion
l_{ref}	=	reference length
M_∞	=	freestream Mach number
N	=	number of samples
P	=	number of variables
Re_j	=	l_{ref}-based Reynolds number
VR	=	jet to local isentropic velocity ratio
V_{inj}	=	injection velocity
$V_{\text{isentropic}}$	=	isentropic boundary velocity
V_x	=	streamwise velocity
V_∞	=	freestream velocity
x_{inj}	=	injection abscissa
y^+	=	normalized first cell height
α	=	angle of attack
δ	=	boundary-layer thickness
δ_{flap}	=	flap deflection angle
δ_{inj}	=	injection angle

I. Introduction

THE requirement for aircraft manufacturers to meet increasingly stringent regulations has pushed industrials and applied researchers toward the in-depth evaluation of innovative design strategies for boundary-layer separation delay or prevention. In this context, active flow control [1–3] is unanimously regarded as a key evolution, offering new solutions for the performance maximization of existing designs, and, to an even greater extent, the apprehension of new concepts, in which it could be used in a multidisciplinary approach, fully integrated to the initial screening and conception phases.

In 1999, McLean et al. [4] examined some of the benefits to be gained from the introduction of unsteady excitation to civil transport aircraft aerodynamics, ranging from exhaust mixing to engine inlet or landing-gear applications. They identified high-lift separation control as one of the most promising and feasible applications through the enhancement of conventional designs [5] or the suppression of slotted flaps. Applying flow control to such cases could not only improve takeoff lift-to-drag ratio and landing maximum lift, but could also result in drastic reductions in radiated noise, mechanical complexity, weight, manufacturing time, and costs from simplifications and/or size reductions relative to current systems.

High-lift devices consisting of simply hinged, moveable slats and/or flaps have had the interest of a growing number of studies in fairly recent years. Seifert et al. [6] conducted wind-tunnel tests on a NACA 0015 airfoil equipped with a 25% chord-length flap deflected up to 40 deg. Actuation in the form of steady/unsteady blowing was applied from a two-dimensional slot located on the suction side of the profile, above the flap pivot. A significant lift augmentation was observed, together with a cancellation of form drag and no adverse effects from Reynolds number increase. The superposition of an unsteady component was also seen to reduce mass flow requirements by 1 order of magnitude compared with steady-only blowing. Nishri and Wygnanski [7] and Darabi and Wygnanski [8,9] experimentally studied flow reattachment over an inclined plane surface simulating a simple flap, with similar conclusions. They reported, however, on the presence of a strong hysteresis effect and, as such, the existence of a dual management scheme (in which it is actually less expensive to maintain an attached flow for increasing flap deflection angles than it is to force reattachment at a given inclination), which ultimately pushes for closed-loop separation control [10]. With the aim of reducing blade–vortex interaction noise in helicopter applications, Hassan [11] performed unsteady thin-layer Navier–Stokes computations over a NACA 0012 airfoil with a 20% chord-length flap, deflected at 40 deg, and equipped with an oscillatory air jet at the upper flap shoulder. Partial flap reattachment was achieved. The author indicates that whereas the importance of transition and turbulence modeling remains of primary concern for Reynolds-averaged Navier–Stokes (RANS)-based simulations of controlled flows, the latter are capable of capturing global flow features with enough fidelity for general aerodynamic trends to be extracted. A parametric study also demonstrated that the expected aerodynamic benefits were mostly dependent on the jet peak Mach number and oscillating frequency (which are intrinsic characteristics of the actuator itself), rather than the injection angle. It is to be noted, however, that these computations do not account for the presence of a cavity below the orifice, which has since been shown to be of fundamental importance for trustworthy comparisons to be made [12].

In a first attempt to combine leading- and trailing-edge separation control, Greenblatt [13] performed experiments on a rectangular

Presented as Paper 4276 at the 25th AIAA Applied Aerodynamics Conference, Miami FL, 25–28 June 2007; received 24 April 2008; revision received 2 February 2009; accepted for publication 8 February 2009.

*Aerospace Engineer, Applied Aerodynamics Department; mickael.meunier@onera.fr.

planform wing equipped with three equal-span flaps hinged at 70% of a NACA 0015 airfoil. Unsteady control is provided by two independently operated bidimensional slots located at the leading edge (and behaving, to some extent, as a conventional leading-edge device) and at the upper flap-shoulder (equivalent to an additional flap deflection) of the wing. An important factor for maximized control efficiency was found in the operating phase shift between each actuator, in which aft suction should be applied when the upcoming shear layer (generated by the forebody excitation) sits closest to the flap surface. The effects of finite span and sweep angle (which is known to affect stall occurrence from an inboard to a tip mechanism in high-lift conditions) were also reported and discussed [14]. Using adapted sweep relations, a simple trajectory model was derived to explain the loss of control effectiveness in the tip region, with leading-edge actuation. Flap-shoulder control yielded some performance improvements, but with a significant loss of efficiency when compared with the unswept case. On the contrary, finite span effects seemed to have little influence against two-dimensional results.

Galbraith [15] performed unsteady RANS (URANS) simulations of the flow around a novel high-lift airfoil with a conventional slotted slat and a simply hinged flap deflected at 40 deg. Separation control was performed via an unsteady surface boundary condition applied near the flap shoulder. A parametric study, interested in the influences of injection angle, frequency, jet velocity average, and amplitude, was presented and discussed for different blowing characteristics (pulsed blowing, pulsed suction, and zero net mass flux). In general, the computations were found to be in good agreement with already available experiments. Lift improvements were reported, but flowfield analysis suggested that a single momentum source might not be capable of fully reattaching the flap flow for reasonable magnitude inputs. In the frame of the Adaptive Flow Control Vehicle Integrated Technologies (ADVINT) program, Kiedaisch et al. [16] conducted two- and three-dimensional (swept wing) experiments on a series of high-lift designs (conventional slotted slat, cruise, and drooped leading edges and slotted or simply hinged flaps), actuated at several locations and backed up by a computational fluid dynamics (CFD) survey by Shmilovich and Yadlin [17] (see also the work by Nagib et al. [18] for a discussion on similarity parameters). To meet their performance goals, the authors suggest that a jet-to-local-velocity ratio beyond two would be required, which could not be achieved for the leading-edge part. On the other hand, the use of active flow control near the flap shoulder, although not capable of complete reattachment, was seen to improve the complete airfoil performance. Eventually, the introduction of a spanwise flow component did not alter flow control efficiency, as also demonstrated by Seifert and Pack [19]. Computational results yielded the same conclusions with favorable comparisons against the experiments. Tests with distributed actuation were performed and showed that the combination of five equally spaced slots operating in phase could fully reattach the flow over the flap.

With the aim of gaining more understanding of the physics governing active control of highly separated flows, Nagib et al. [20] performed a numerical study on the same range of configurations. The authors identified four interdependent mechanisms as being responsible for lift enhancement: namely, separation and circulation controls, thrust vectoring of the active actuation, and surface pressure manipulation up to, and above, inviscid levels. In a companion series of small-scale experiments, Kiedaisch et al. [21] examined the influence of the dynamic deflection of a drooped flap and concluded on the independence of actuation effects on deflection rate, up to the angle at which separation could not be fully alleviated anymore and for which static control outperformed the dynamic one.

In a series of publications, Pack Melton et al. [22–24] presented wind-tunnel measurements on a supercritical airfoil fitted with a 15 and 25% chord length simply hinged slat and flap. Synthetic control was applied at several leading- and trailing-edge positions, and tests with combined actuated locations were performed. Overall, it was found that larger momentum inputs are required for an effective management of the flap separation (when compared with the slat counterpart), with emphasis put on the importance of surface curvature. Encouraging results were also reported from synchronous fore and aft excitations. Khodadoust and Washburn [25] and Khodadoust and Shmilovich [26] presented a combined experimental/computational study of the same airfoil equipped with a slotted flap (in lieu of the simply hinged one) at higher Reynolds numbers (up to 9×10^6). The effect of that last parameter was found to be significant indeed, suggesting that the assessment of control performance be conducted at near flight-scale conditions. Furthermore, and without looking at actuation power requirements, steady active control provided better maximum lift increments than zero-mass-flux input. Again, a satisfactory agreement is reported between wind-tunnel tests and simulations, specifically in the linear lift range.

Although appealing, the suppression of the slat and flap slots is not as easy as it would originally appear. They are important elements in which the entire performance of conventional high-lift configurations are to be found [27], from limitations to local pressure rises (the primary cause of flow separation) and a more homogeneous repartition of the airfoil loads over its three (or more) elements. Adding the presence of rapid and rather severe geometry changes to the loss of these highly elliptical effects, it is easy to understand that the aerodynamic behavior of uncontrolled slotless geometries is relatively poor in its original basis, being subject to massive separations and early stall.

Although the preceding investigations demonstrate various degrees of improvements from the introduction of flow control concepts, the sensitivity of aerodynamic performance to design choices makes it a nontrivial and certainly expensive problem, the number of actuation parameters and combinations thereof being almost infinite. As a possible answer [28,29], a completely automated, surrogate-based optimization [30,31] algorithm was developed and applied to the design of a two-dimensional high-lift system with a conventional slotted slat and a simply hinged, slotless flap. The process will now be described in detail and results for a continuously blowing slot will be presented.

II. Overview of the Optimization Process

A general flowchart for any surrogate-based optimization loop is presented in Fig. 1. Details for each individual procedure are given in the following sections. The framework of this algorithm, which has been extensively validated over a series of analytical test

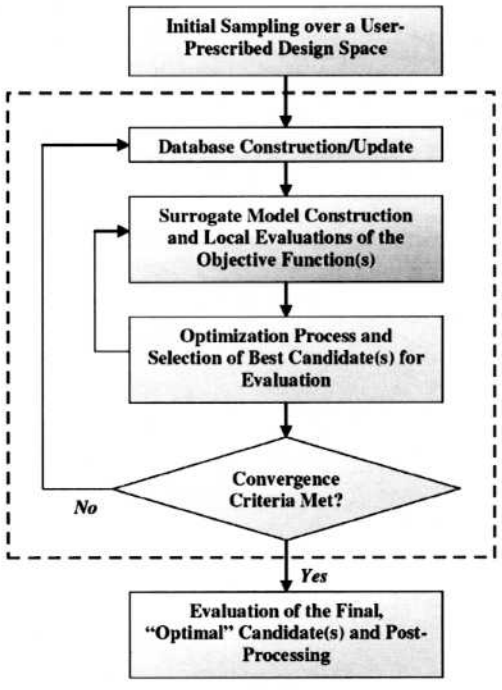

Fig. 1 Outline of surrogate-based optimization algorithms.

problems (see [32] for corresponding complements), is a collection of FORTRAN/Shell routines encompassed in a Python computer language interface.

A. Sampling

The construction of a surrogate model of any black-box function requires the creation of a database of precisely evaluated individuals. By database, we mean a collection of samples, spread all over or slightly outside the design space of interest, which should be as representative as possible of the interactions existing between the design variables on the one side and the objective functions to be optimized on the other side. It is of fundamental importance for the sampled points to be distributed homogeneously across the search space so that no region is left without a single representative. The apparition of design-of-experiments concepts has introduced a large number of sampling methods, including fully random, Monte Carlo, Tagushi, Halton/Hammersley, central Voronoï tessellation, or Latin hypercube, each with its advantages and drawbacks [33,34]. Among these, the constrained space-filling Latin hypercube sampling (LHS) was chosen for its simplicity and yet good overall performance compared with other, more complex, formulations. In the case in which we wish to gather N samples of P variables [where $N \geq (3 \text{ to } 10)^P$ is a first rule of thumb for a correct initial representation], the LHS strategy is performed as follows:

1) Divide the range of each variable into N nonoverlapping equal-probability (hence equal-size) intervals.

2) From a user-specified (usually uniform) probability density, arbitrarily select one value from each interval in every direction and randomly couple (equally likely combinations) the N values of each dimension.

B. Design Analyzer: RANS CFD Flow Solver

The computational method used in this study relies on ONERA's structured, multiblock, cell-centered, elsA CFD software [35]. The Reynolds-averaged form of the Navier–Stokes equations is solved using the Jameson et al. [36] second-order centered scheme with artificial viscosity for the spatial discretization. The implicit phase is resolved using a lower/upper symmetric successive over-relaxation technique, and convergence is accelerated through a one-level, v-cycle, multigrid algorithm combined with low-speed preconditioning. Turbulence closure is achieved under a Boussinesq hypothesis using the one-equation model of Spalart and Allmaras (SA) [37]. Precise, fully turbulent, boundary-layer resolutions ensured average y^+ (based on the height of the first wall-bounded cell) values below unity for all of the meshes considered here. To keep the overall computational cost of the procedure as reasonable as possible, and bearing in mind that design definitions based on automated optimization are concerned mainly with precise trends and performance variations between each design point (rather than their precise performance assessment, as such, provided that the correct physics of the phenomena to be modeled is effectively captured), steady-state solutions were obtained using a quasi-stationary backward-Euler integration with a Courant–Friedrichs–Lewy number-derived time step. For all cases, a thorough iterative convergence study (on residuals, forces, and moments) guaranteed that fully converged solutions were obtained. The prediction capabilities of the software for isolated [38] and flow-control-enhanced [5] high-lift problems have been reported already and will not be further discussed here.

C. Surrogate Model (Response Surface Method)

The major disadvantage of classical optimization techniques is the important computational cost of the high-fidelity analyzer at each objective-function evaluation. An alternative is the construction of a response model that links the design variables with the inputs for the optimizer (i.e., objective functions) through a simple and inexpensive, yet accurate, relation. The most widely used substitute models include multilayer perceptron or radial basis functions [39] neural networks, polynomial-based formulations, and, gaining increasing popularity, the kriging linear interpolation method, as formulated in its ordinary form by Sacks et al. [40].

Let us consider a globally unknown function Y, expressed as a stochastic process:

$$Y(x) = \beta + Z(x) \tag{1}$$

where x is the P-dimensional vector of design variables; β is a global constant of the model (its mean); and $Z(x)$ represents an error, or deviation, term assumed to have mean zero and covariance (COV)

$$\text{COV}\,(Z(x_i), Z(x_j)) = \sigma^2 \cdot R(f(x_i, x_j)) \tag{2}$$

between $Z(x_i)$ and $Z(x_j)$, where σ^2 is the process variance and R a symmetric, $N \times N$ correlation matrix with ones along the diagonal. The strongest hypothesis of this method if the choice of f as a user-specified, predefined, correlation function.

To estimate the random components of Y, the N original (LHS) sample points are interpolated using a Gaussian correlation function. This makes them closely dependent on the relative distance between each design sites, $d(x_i, x_j)$. Instead of an Euclidian distance, that would weight all the variables equally, the following norm is employed:

$$d(x_i, x_j) = \prod_{k=1}^{P} \theta^k \cdot |x_i^k - x_j^k|^2 \tag{3}$$

where $\theta^k > 0$ is a correlation parameter vector, or, if deemed sufficient constant (as in the case here, hence the isotropic nature of the surrogate) to be determined.

Based on that, the Gaussian correlation function between the errors at x_i and x_j becomes

$$f(x_i, x_j) = e^{-d(x_i, x_j)} \tag{4}$$

Now, let r denote the N vector of correlations between the estimation error at x^*, an untried design set, and the error terms at the already known points.

The derivation of the kriging predictor, not discussed here, yields the following estimation of Y (marked $\hat{y}$) at x^*:

$$\hat{y}(x^*) = \hat{\beta} + r^T.R^{-1}.(y - 1.\hat{\beta}) \tag{5}$$

where $\hat{\beta}$ is an estimation of β and y the true value of Y at each sampling point. The determination of the $P + 2$ unknown parameters $(\theta, \beta, \sigma^2)$ is such that they maximize the log-likelihood of the samples: that is, the log form of the maximum likelihood function (MLF) defined as

$$\text{MLF} = \max_{\theta,\beta,\sigma^2}\left[-\frac{N}{2}\cdot \ell_n(\sigma^2) - \frac{1}{2}\cdot \ell_n(|R|) - \frac{-(y - 1\cdot\beta)^T \cdot R^{-1} \cdot (y - 1\cdot\beta)}{2\cdot\sigma^2}\right] \tag{6}$$

The corresponding estimates of β and σ^2 are

$$\hat{\beta} = \frac{1^T \cdot R^{-1} \cdot y}{1^T \cdot R^{-1} \cdot 1} \quad \text{and} \quad \hat{\sigma}^2 = \frac{(y - 1\cdot\hat{\beta})^T \cdot R^{-1} \cdot (y - 1\cdot\hat{\beta})}{N} \tag{7}$$

The preceding problem, dependent only on θ, is solved using the same unconstrained nonlinear optimization technique as employed for the global problem and described subsequently.

The quality of the prediction is obviously affected by the correlation of the errors, that is the distance between x^* and the reference points (the closer, the better). This is expressed in the following expression for root-mean-square prediction error (RMSE):

$$s(x^*) = \hat{\sigma}\cdot\left[1 - r^T \cdot R^{-1} \cdot r + \frac{(1 - 1^T \cdot R^{-1} \cdot r)^2}{1^T \cdot R^{-1} \cdot 1}\right]^{1/2} \tag{8}$$

Thus, a kriging interpolation is able to provide both an estimation of the objective function and some sort of uncertainty quantification